


# Model free sliding mode stabilizing control of a real rotary inverted pendulum

İlhami Yiğit

Journal of Vibration and Control  
1–18  
© The Author(s) 2015  
Reprints and permissions:  
sagepub.co.uk/journalsPermissions.nav  
DOI: 10.1177/1077546315598031  
jvc.sagepub.com  


## Abstract

Inverted pendulum systems, because of highly nonlinear, coupled, and unstable dynamic behaviour, are excellent experimental platforms for testing new developed control algorithms. This study explores nonlinear modelling, simulation and sliding mode stabilizing control of a real rotary inverted pendulum in detail. For simulation purposes only, the system was modelled in a nonlinear state space form including the servomotor dynamics. In the light of the simulation results, a rotary inverted pendulum system was designed and manufactured. For a certain quality level of desired output, benefits of the sliding mode control of the system without using an equivalent control signal by selecting a proper smoothing function were shown. This model free approach can be used to satisfy a need especially for practical control applications in industry to a certain level, encouraging practical control engineers to use sliding mode control, who have no ability to model a system or no sufficient time for this, or encounter very complex nonlinear system models in many cases. Comparisons of the theoretical and experimental results demonstrate that the state equations describe the dynamics of the system satisfactorily, and that robust and accurate balancing of the pendulum can be achieved by using model free sliding mode control with sigmoid smoothing function.

## Keywords

Rotary inverted pendulum, sliding mode control, nonlinear modelling, simulation, experiment

## 1. Introduction

Due to the highly nonlinear, coupled, and unstable dynamic behaviour, inverted pendulum systems are excellent experimental platforms for testing new developed control algorithms, especially in nonlinear control and comparing them with older ones, and for educational purposes in most control laboratories. Their applications correspond to several modern systems in real world such as walking robots, space shuttle guidance systems with side jets, satellite guidance and control systems, cranes at construction sites, etc (Olfati-Saber, 2000). Most rotary inverted pendulums consist of a horizontal link rotating about a vertical axis to balance a second link which is connected to the end of first link with a revolute joint, thus having two degrees of freedom. The first link is driven by a motor and rotates in the horizontal plane to swing-up and balance a pendulum link rotating freely in the vertical plane. Since the second link is arm-driven only, the system is underactuated (Figure 1). Rotary inverted pendulums are also very preferable inverted pendulum systems and perfect test beds to study on controlling the underactuated, nonlinear and

unstable systems (Åström and Furuta, 2000; KRi, 2015; Khanesar et al., 2007; Anvar et al., 2010). Their constructions are comparatively simpler, easier and more precise than cart-type inverted pendulums as they possess only revolute joints and using direct drive. Besides, their nonlinearity, dynamic behaviour and coupling are preferably more complex than the cart-type inverted pendulums.

There are four types of control task such as i) swinging up from its stable pending position to the upright unstable position, ii) catching the pendulum around stable upright position, iii) balancing (stabilizing) the pendulum at the upright position in spite of disturbances, and iv) holding the horizontal link to a specified

Department of Mechanical Engineering, Faculty of Engineering and Architecture, Bozok University, Yozgat, Turkey

Received: 10 November 2014; accepted: 4 July 2015

### Corresponding author:

İlhami Yiğit, Department of Mechanical Engineering, Faculty of Engineering and Architecture, Bozok University, Yozgat 66100, Turkey.  
Email: yigitil@yahoo.com

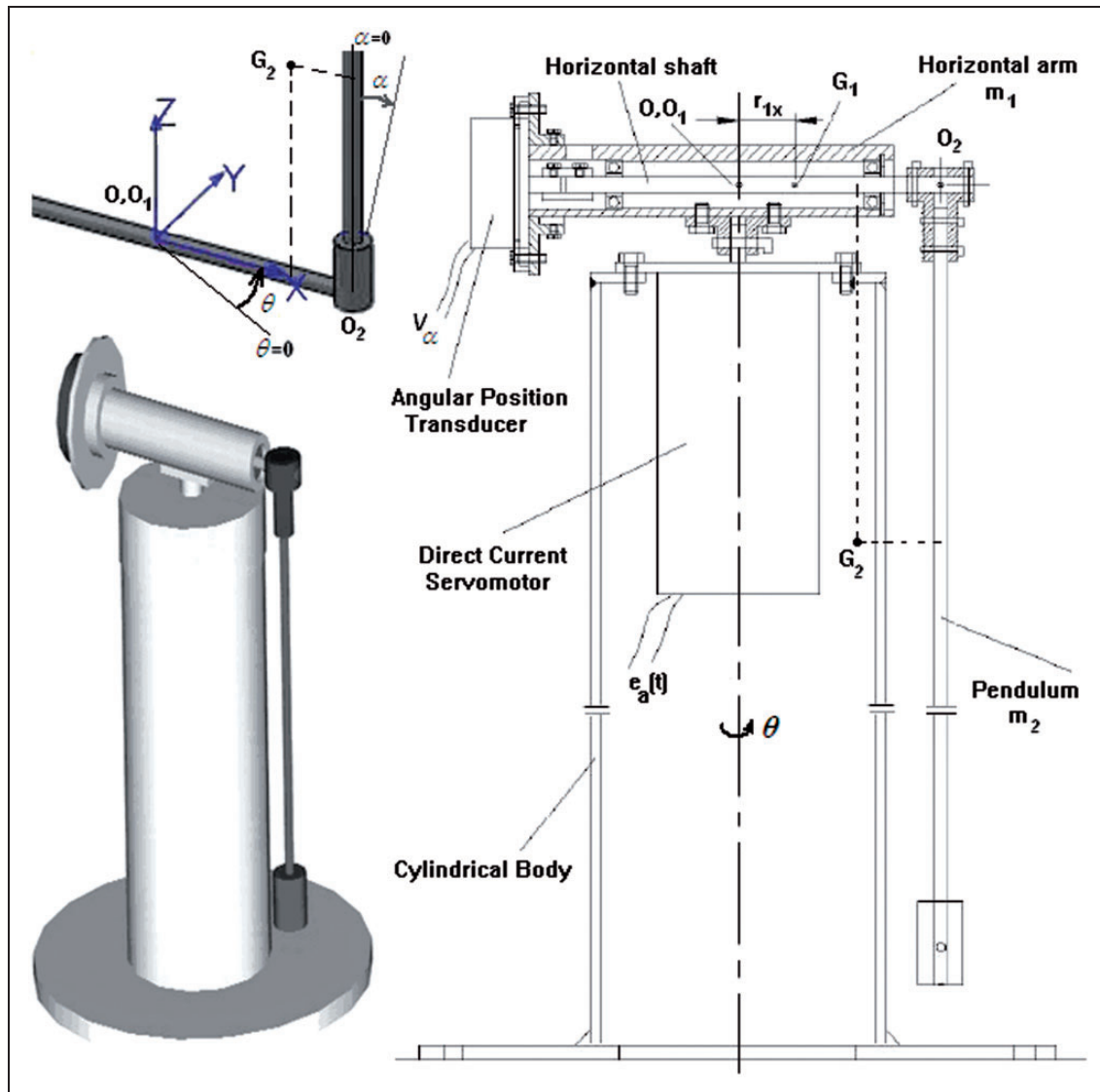


**Figure 1.** The rotary inverted pendulum system developed.

angular position with the pendulum balanced at upright position (KRi, 2015). This paper deals with only catching and balancing the pendulum at the upright position in spite of disturbances in detail. Many techniques for catching and balancing of an inverted pendulum have been proposed in the literature (Awtar et al., 2002; Chih-Jer et al., 2003; KRi, 2015). In this study, classical PID control and sliding mode control (SMC) techniques were used on a real inverted pendulum. In order to make comparisons and observe its performance clearly, first PID control and then model free SMC were applied to the system.

The kinematic analysis of the system was made as in an analysis of a two degrees of freedom robot manipulator. Lagrangian formulations were used to obtain dynamic behaviour of the system in the present study.

It is recommended that the readers refer to Pakdeepattarakorn et al. (2004), Berg (2003) and Awtar et al. (2002) for some different aspects of the derivation of the system model.

The system was represented in a nonlinear state space form including the servomotor dynamics in contrast to many research studies (Olfati-Saber, 2000; Chih-Jer et al., 2003; Anvar et al., 2010; Khanesar et al., 2007). As shown in these studies, neglecting the servomotor dynamics (assuming an algebraic expression or only using a control torque  $u$ ) makes it possible to obtain an equivalent control easily. However, in many cases, for a precise control, the transient response of a servomotor could not be neglected in high frequency control systems like an inverted pendulum, because the motor has to run mostly in its transient

area even if it has a small terminal inductance. An equivalent control found in this way is already an approximate control signal.

For simulation purposes only, the system was modelled in a nonlinear state space form including the servomotor dynamics. A great number of simulations were implemented to know the system thoroughly. In the light of the simulation results, a rotary inverted pendulum was specially designed and manufactured. Most parameters of the pendulum system were determined experimentally by accurate methods. Simulation studies were repeated with the real system parameters. In this study, since the control aim is to balance the pendulum at upright unstable position, only the angular position of the pendulum is measured and fed back. Control variable is angular position of the pendulum. Plant input is the applied voltage to the servomotor. Desired values of the pendulum angle and the disturbances are the inputs to the closed loop control system. In simulation and experimental studies, several performance tests were implemented in order to show the efficiency of the utilized control technique and overall performance of the pendulum system developed, using PD control, PID control, SMC with *sat* saturation function and SMC with *tanh* sigmoid smoothing functions (hyperbolic tangent function) to avoid chattering.

In this study, for a desired quality in output, benefits of the SMC of the system without using an equivalent control signal using a proper smoothing function were shown. This model free approach (Utkin, 1994) can be used to meet a need especially for practical control applications in a wide range of industry, encouraging practical control engineers to use SMC, who have no ability of modelling a system or no sufficient time for this, or encounter very complex nonlinear system models in many cases. To obtain an exact equivalent control requires a perfect system model (i.e., without neglecting the servomotor dynamics and considering uncertainties, etc), full state feedback, solution of nonlinear equations analytically, and a properly chosen Lyapunov candidate function for stability analysis. It means that an equivalent control signal can only be obtained approximately. Besides, it was shown in Trivedi and Bandyopadhyay (2010) that “the equivalent control can be non unique” in contrast to knowledge in literature. Due to these difficulties, research studies on estimating the equivalent control are gradually increasing (Utkin, 1992; Usai, 2008; Fridman, 2012). Hence, in many cases, SMC without an equivalent control signal can easily meet the needs in practical control areas to a certain level, depending on the desired quality of the output.

In conclusion, comparisons of the theoretical and experimental results demonstrate that the state

equations describe the dynamic behaviour of the system satisfactorily, and that robust and accurate balancing control of the pendulum can be achieved by using model free SMC with sigmoid smoothing function.

## 2. Modelling of the system

In this section, physical and mathematical model of the system will be dealt with in detail. Then, the state equations of the system will be given in standard form.

### 2.1. Physical model

The inverted pendulum system developed (Figure 1) consists of the following main mechanical parts: a cylindrical main body, a permanent magnet brushed direct current (dc) servomotor, horizontal arm (first link) driven by the motor, the pendulum (second link) on the end of the first link with a revolute joint - with an adjustable mass on its end, ball bearings, and a measurement potentiometer for angular position of the pendulum.

Control signal from the computer (PC) is a low level voltage signal and cannot be used to drive the servomotor. Therefore, an adjustable gain push-pull servo amplifier was used to convert the voltage output of the PC to a higher voltage signal, together with the current boosting according to the need.

### 2.2. Mathematical model

**2.2.1. Equations of motion.** The kinematic analysis of the system was made as in an analysis of a two degrees of freedom robot manipulator. Lagrangian formulations were used to obtain dynamic behaviour of the system in the present study. It is recommended that the readers refer to Pakdeepattarakorn et al. (2004), Berg (2003) and Awtar et al. (2002) for some different aspects of the derivation of the system model. Figure 1 shows the origins of the moving coordinate frames coinciding with the links, the lengths and the centre of gravities (CG) of the links. The main coordinate frame  $Oxyz$ , the moving coordinate frames  $Ox_1y_1z_1$  of the first link (horizontal arm) and  $Ox_2y_2z_2$  of the second link (pendulum) are shown in Figure 2. The axes  $z$  and  $z_1$  coincide with the motor shaft and in upward positive direction. The  $z_2$  axis coincides with the pendulum and in upward positive direction while the pendulum is at stable pending position.

The lengths of the links and the center of gravities:

$l_2$  : length of the pendulum (m)

$r_{1x}$  : horizontal component of the position vector  $O$  to CG of the horizontal arm (m)

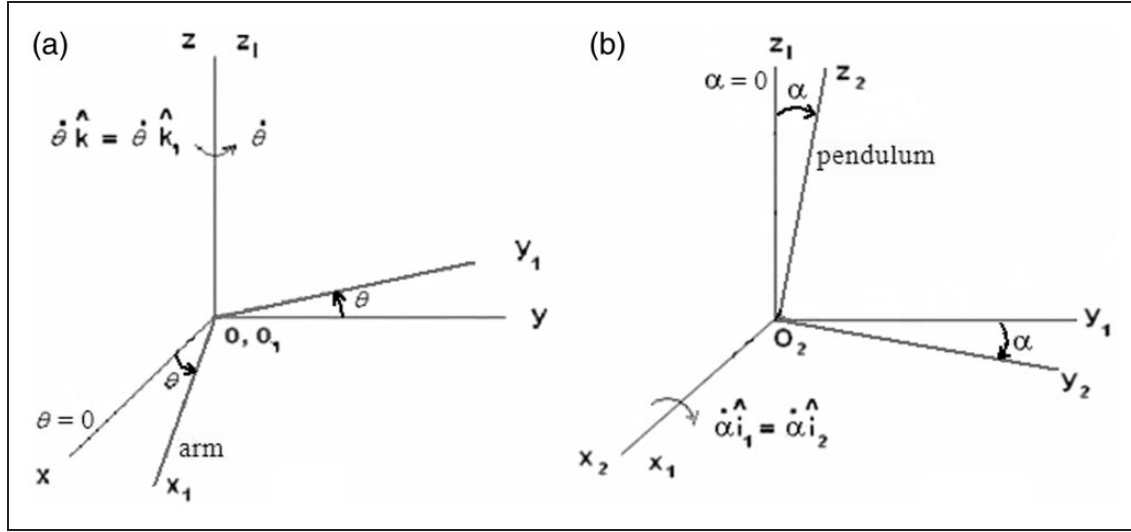


**Figure 2.** Moving coordinate frames: a)  $Ox_1y_1z_1$  of the arm and b)  $Ox_2y_2z_2$  of the pendulum.

$r_{12}$  : distance from origin  $O_1$  to origin  $O_2$  (m)

$r_{2x}$  : horizontal component of the position vector from origin  $O$  to CG of the pendulum (m)

$r_{2z}$  : vertical component of the position vector from origin  $O$  to CG of the pendulum (m)

Reference coordinate frames:

$R$  :  $Oxyz$  coordinate frame

$R_1$  :  $Ox_1y_1z_1$  coordinate frame

$R_2$  :  $Ox_2y_2z_2$  coordinate frame

$\theta, \dot{\theta}$  : angular position and velocity of the arm around  $z$  or  $z_1$  axis (rad, rad/s)

$\alpha, \dot{\alpha}$  : angular position and velocity of the pendulum around  $x_1$  or  $x_2$  axis (rad, rad/s)

$\hat{i}_n, \hat{j}_n$  and  $\hat{k}_n$ ;  $n = 1, 2, 3$  : unit vectors of the  $n$  th coordinate frame, depicted with caps

Coordinate transformation matrices:

$$\begin{bmatrix} \hat{i}_1 \\ \hat{j}_1 \\ \hat{k}_1 \end{bmatrix} = \begin{bmatrix} \cos \theta & \sin \theta & 0 \\ -\sin \theta & \cos \theta & 0 \\ 0 & 0 & 1 \end{bmatrix} \begin{bmatrix} \hat{i} \\ \hat{j} \\ \hat{k} \end{bmatrix}$$

$$\& \begin{bmatrix} \hat{i}_2 \\ \hat{j}_2 \\ \hat{k}_2 \end{bmatrix} = \begin{bmatrix} 1 & 0 & 0 \\ 0 & \cos \alpha & -\sin \alpha \\ 0 & \sin \alpha & \cos \alpha \end{bmatrix} \begin{bmatrix} \hat{i}_1 \\ \hat{j}_1 \\ \hat{k}_1 \end{bmatrix}$$

Masses and mass moment of inertias of the arm and the pendulum:

$m_1$  : mass of the arm (kg)

$m_2$  : mass of the pendulum (kg)

$I_{1z}$  : moment of inertia of the arm plus rotor inertia of the motor with respect to (wrt)  $z$ -axis ( $\text{kg.m}^2$ )

$I_2$  : tensor of the moment of inertias of the pendulum wrt the center of gravity  $G_2$  ( $\text{kg.m}^2$ )

$$I_2 = \begin{bmatrix} I_{2x} & I_{2xy} & I_{2xz} \\ I_{2yx} & I_{2y} & I_{2yz} \\ I_{2zx} & I_{2zy} & I_{2z} \end{bmatrix}$$

Position vectors of the center of gravities of the arm and the pendulum wrt  $Oxyz$  coordinate frame can be stated as follows:

$$\vec{r}_{G_1} = \vec{OG}_1 = r_{1x} \hat{i}_1 = r_{1x} \cos \theta \hat{i} + r_{1x} \sin \theta \hat{j} \quad (1)$$

$$\begin{aligned} \vec{r}_{G_2} = \vec{OG}_2 = & r_{2x} \hat{i}_1 + r_{2z} \hat{k}_2 = (r_{2x} \cos \theta - r_{2z} \sin \theta \sin \alpha) \hat{i} \\ & + (r_{2x} \sin \theta + r_{2z} \cos \theta \sin \alpha) \hat{j} + (r_{2z} \cos \alpha) \hat{k} \end{aligned} \quad (2)$$

Velocity vectors of the center of gravities of the arm and the pendulum wrt  $Oxyz$  coordinate frame can be found by taking time derivative of the position vectors wrt  $Oxyz$ .

$$\vec{v}_{G_1} = -r_{1x} \dot{\theta} \sin \theta \hat{i} + r_{1x} \dot{\theta} \cos \theta \hat{j} \quad (3)$$

$$\begin{aligned} \vec{v}_{G_2} = & (-r_{2x} \dot{\theta} \sin \theta - r_{2z} \dot{\alpha} \sin \theta \cos \alpha - r_{2z} \dot{\theta} \cos \theta \sin \alpha) \hat{i} \\ & + (r_{2x} \dot{\theta} \cos \theta - r_{2z} \dot{\theta} \sin \theta \sin \alpha + r_{2z} \dot{\alpha} \cos \theta \cos \alpha) \hat{j} \\ & + (-r_{2z} \dot{\alpha} \sin \alpha) \hat{k} \end{aligned} \quad (4)$$

Angular velocity vectors of the arm and the pendulum wrt  $Oxyz$  coordinate frame can be written as

$$\vec{\omega}_{arm} = \dot{\theta} \hat{k}_1 = \dot{\theta} \hat{k} \quad (5)$$

$$\vec{\omega}_{pend} = \dot{\theta} \hat{k} + \dot{\alpha} \hat{i}_1 = (-\dot{\alpha} \cos \alpha) \hat{i} + (-\dot{\alpha} \sin \alpha) \hat{j} + (\dot{\theta}) \hat{k} \quad (6)$$

Lagrangian formulations require kinetic and potential energies of the system. Kinetic energy of the arm can be obtained in terms of the angular momentum of the arm as

$$T_{arm} = \frac{1}{2} \vec{\omega}_{arm}^T \vec{H}_{arm} = \frac{1}{2} \vec{\omega}_{arm}^T I_{arm} \vec{\omega}_{arm} = \frac{1}{2} I_{1z} \dot{\theta}^2 \quad (7)$$

where  $I_{arm} = I_1$  and only  $I_{1z}$  element of the matrix is different from zero.

Kinetic energy of the pendulum:

$$T_{pend} = T_{trans} + T_{rot} = \frac{1}{2} m_2 \vec{v}_{G_2} \cdot \vec{v}_{G_2} + \frac{1}{2} \vec{\omega}_{pend}^T \vec{H}_{pend} \quad (8)$$

where

$$\begin{aligned} \vec{v}_{G_2} \cdot \vec{v}_{G_2} &= v_{G_2}^2 = v_{G_{2x}}^2 + v_{G_{2y}}^2 + v_{G_{2z}}^2 \\ &= (r_{2x}^2 + r_{2z}^2 \sin^2 \alpha) \dot{\theta}^2 + (2r_{2x} r_{2z}) \dot{\theta} \dot{\alpha} + (r_{2z}^2) \dot{\alpha}^2 \end{aligned} \quad (9)$$

$H_{pend}$  is the angular momentum of the pendulum wrt  $Oxyz$  and can be calculated in terms of inertia tensor and angular velocity of the pendulum as given below.

$$\vec{H}_{pend} = I_2 \vec{\omega}_{pend} = \begin{bmatrix} I_{2x} & I_{2xy} & I_{2xz} \\ I_{2yx} & I_{2y} & I_{2yz} \\ I_{2zx} & I_{2zy} & I_{2z} \end{bmatrix} \begin{bmatrix} \omega_x \\ \omega_y \\ \omega_z \end{bmatrix} \quad (10)$$

Based on Figure 1, inertia tensor of the pendulum was obtained using SolidWorks CAD Program (solid modelling) such that  $I_{2xy} = I_{2yx} = 0$  and  $I_{2yz} = I_{2zy} = 0$ . Therefore, angular momentum vector of the pendulum wrt  $Oxyz$  can be written as

$$\vec{H}_{pend} = (I_{2x} \omega_x + I_{2xz} \omega_z) \hat{i} + (I_{2y} \omega_y) \hat{j} + (I_{2xz} \omega_x + I_{2z} \omega_z) \hat{k} \quad (11)$$

Thus, total kinetic energy of the system can be found as

$$\begin{aligned} T &= \frac{1}{2} m_2 \left[ (r_{2x}^2 + r_{2z}^2 \sin^2 \alpha) \dot{\theta}^2 + (2r_{2x} r_{2z}) \dot{\theta} \dot{\alpha} + (r_{2z}^2) \dot{\alpha}^2 \right] \\ &+ \frac{1}{2} (I_{2x} \dot{\alpha}^2 \cos^2 \theta + I_{2y} \dot{\alpha}^2 \sin^2 \theta + I_{2z} \dot{\theta}^2 + 2I_{2xz} \dot{\theta} \dot{\alpha} \cos \theta) \end{aligned} \quad (12)$$

Total potential energy of the system taking the horizontal plane passing through origin  $O$  as reference plane can be stated as follows: (taking  $g = 9.81 \text{ m/s}^2$ )

$$V = V_{arm} + V_{pend} = 0 + m_2 g r_{2z} \cos \alpha = m_2 g r_{2z} \cos \alpha \quad (13)$$

Thus, Lagrangian of the system ( $L = T - V$ ) can be obtained as follows:

$$\begin{aligned} L &= \frac{1}{2} m_2 \left[ (r_{2x}^2 + r_{2z}^2 \sin^2 \alpha) \dot{\theta}^2 + (2r_{2x} r_{2z}) \dot{\theta} \dot{\alpha} + (r_{2z}^2) \dot{\alpha}^2 \right] \\ &+ \frac{1}{2} (I_{2x} \dot{\alpha}^2 \cos^2 \theta + I_{2y} \dot{\alpha}^2 \sin^2 \theta + I_{2z} \dot{\theta}^2 + 2I_{2xz} \dot{\theta} \dot{\alpha} \cos \theta) \\ &- m_2 g r_{2z} \cos \alpha \end{aligned} \quad (14)$$

In order to obtain the dynamic behaviour of the system the Lagrangian formulation are used for dynamic analysis as stated below.

$$\frac{d}{dt} \left[ \frac{\partial L}{\partial \dot{q}_i} \right] - \frac{\partial L}{\partial q_i} = Q_i \quad (15)$$

where

$q_i, Q_i$ : generalized coordinates and forces, respectively.  
( $q_1 = \theta$  &  $q_2 = \alpha$ ;  $Q_i, i = 1, 2$ )

$$Q_1 = M_{motor}(t) - M_{sa} - M_{ba}(t) \quad (16)$$

$$Q_2 = -M_{sp} - M_{bp}(t) \quad (17)$$

$M_{motor}(t)$ : torque generated by the motor (N·m)

$M_{sa}$ : viscous and Coulomb friction moments about rotation axis of the arm

$M_{sp}$ : viscous and Coulomb friction moments about rotation axis of the pendulum

$M_{ba}(t)$ : disturbance moment acting on the arm

$M_{bp}(t)$ : disturbance moment acting on the pendulum

$$M_{sa} = B_a \dot{\theta} + M_{fa} \text{sgn}(\dot{\theta}) \quad (18)$$

$$M_{sp} = B_p \dot{\theta} + M_{fp} \text{sgn}(\dot{\alpha}) \quad (19)$$

$B_a, B_p$  : viscous damping coefficients, during  $\theta$  and  $\alpha$  rotations of the arms, respectively  
 $M_{fa}, M_{fp}$  : Coulomb friction moments, during  $\theta$  and  $\alpha$  rotations of the arms, respectively  
 $\text{sgn}(x)$  : sign function ( equals 1, 0 and -1; if  $x$  is positive, zero and negative, respectively)

Applying equation (15) for the arm and the pendulum, following equations of motion are obtained.

$$\begin{aligned} & [I_{1z} + m_2 r_{2x}^2 + m_2 r_{2z}^2 \sin^2 \alpha + I_{2z}] \ddot{\theta} + [m_2 r_{2x} r_{2z} \cos \alpha \\ & + I_{2xz} \cos \theta] \ddot{\alpha} + [2m_2 r_{2z}^2 \sin \alpha \cos \alpha] \dot{\alpha} \dot{\theta} \\ & + [m_2 r_{2x} r_{2z} \sin \alpha + I_{2x} \sin \theta \cos \theta - I_{2y} \sin \theta \cos \theta] \dot{\alpha}^2 \\ & = M_{motor}(t) - B_a \dot{\theta} - M_{fa} \text{sgn}(\dot{\theta}) - M_{ba}(t) \end{aligned} \quad (20)$$

$$\begin{aligned} & [m_2 r_{1x} r_{2z} \cos \alpha + I_{2xz} \cos \theta] \ddot{\theta} + [m_2 r_{2z}^2 + I_{2x} \cos^2 \theta] \ddot{\alpha} \\ & + [-m_2 r_{2z}^2 \sin \alpha \cos \alpha - I_{2z} \sin \theta] \dot{\theta}^2 \\ & + [-2I_{2x} \sin \theta \cos \theta + 2I_{2y} \sin \theta \cos \theta] \dot{\theta} \dot{\alpha} \\ & + m_2 g l_{21} \sin \alpha = B_p \dot{\alpha} - M_{fp} \text{sgn}(\dot{\alpha}) - M_{bp}(t) \end{aligned} \quad (21)$$

The system was represented in a nonlinear state space form as shown in the state space representation, including the servomotor dynamics in contrast to many research studies (Olfati-Saber, 2000; Chih-Jer et al., 2003; Anvar et al., 2010; Khanesar et al., 2007).

**2.2.2. State space representation.** Taking  $x_1 = \theta$ ,  $x_2 = \dot{\theta}$ ,  $x_3 = \alpha$  and  $x_4 = \dot{\alpha}$ , Equations. 20 and 21 can be written in a simplified form as follows:

$$C_1 \ddot{\theta} + C_2 \ddot{\alpha} = R_{12} \quad (22)$$

$$C_5 \ddot{\theta} + C_6 \ddot{\alpha} = R_{56} \quad (23)$$

where

$$\begin{aligned} R_{12} = & -C_3 x_4^2 - C_4 x_2 x_4 + M_{motor}(t) - B_a x_2 \\ & - M_{fa} \text{sgn}(x_2) - M_{ba}(t) \end{aligned}$$

$$\begin{aligned} R_{56} = & -C_7 x_2^2 - C_8 x_2 x_4 - m_2 g l_{21} \sin x_3 \\ & - B_p x_4 - M_{fp} \text{sgn}(x_4) - M_{bp}(t) \end{aligned}$$

$$C_1 = I_{1z} + m_2 r_{2x}^2 + m_2 r_{2z}^2 \sin^2 \alpha + I_{2z}$$

$$C_2 = m_2 r_{2x} r_{2z} \cos \alpha + I_{2xz} \cos \theta$$

$$C_3 = m_2 r_{2x} r_{2z} \sin \alpha + I_{2x} \sin \theta \cos \theta - I_{2y} \sin \theta \cos \theta$$

$$C_4 = 2m_2 r_{2z}^2 \sin \alpha \cos \alpha$$

$$C_5 = m_2 r_{1x} r_{2z} \cos \alpha + I_{2xz} \cos \theta$$

$$C_6 = m_2 r_{2z}^2 + I_{2x} \cos^2 \theta$$

$$C_7 = -m_2 r_{2z}^2 \sin \alpha \cos \alpha - I_{2z} \sin \theta$$

$$C_8 = -2I_{2x} \sin \theta \cos \theta + 2I_{2y} \sin \theta \cos \theta$$

If equations (22) and (23) are solved together for  $\dot{z}_2 = \ddot{\theta}$  and  $\dot{z}_4 = \ddot{\alpha}$  and the servomotor dynamics (Eker, 2006; Ogata, 1997) is added into the state equations obtained with the following equations:

$$\frac{di_m}{dt} = \left( \frac{-R_m}{L_m} \right) i_m + \left( \frac{-K_e}{L_m} \right) \omega_m + \left( \frac{1}{L_m} \right) e_a(t) \quad (24)$$

$$M_{motor}(t) = K_t i_m \quad (25)$$

and taking  $x_5 = i_m$ , then state equations of the system to be controlled (plant) are obtained as follows in a standard form.

$$\dot{x}_1 = x_2 \quad (26)$$

$$\dot{x}_2 = [C_6 R'_{12} - C_2 R_{56}] / [C_1 C_6 - C_2 C_5] \quad (27)$$

$$\dot{x}_3 = x_4 \quad (28)$$

$$\dot{x}_4 = [C_1 R_{56} - C_5 R'_{12}] / [C_1 C_6 - C_2 C_5] \quad (29)$$

$$\dot{x}_5 = \left( \frac{-K_e}{L_m} \right) x_2 + \left( \frac{-R_m}{L_m} \right) x_5 + \left( \frac{1}{L_m} \right) e_a(t) \quad (30)$$

where

$$\begin{aligned} R'_{12} = & -C_3 x_4^2 - C_4 x_2 x_4 + K_t x_5 - B_a x_2 \\ & - M_{fa} \text{sgn}(x_2) - M_{ba}(t) \end{aligned}$$

$e_a(t)$  : voltage applied to the motor (Volt, V)

$i_m$  : current through the motor bobbins (Ampere, A)

$R_m$  : terminal resistance of the motor (Ohm,  $\Omega$ )

$L_m$  : terminal inductance of the motor (Henry, H)

$K_e$  : back e.m.f. constant (Volt.s/rad)

$K_t$  : torque constant ( $= K_e$ ), (N.m/A)

As shown in equations (22) to (30), rotary inverted pendulum exhibits highly nonlinear, coupled, and unstable dynamic behaviour. Inputs to the plant are the voltage applied to the servomotor and the disturbance in the form of moments that are applied to the pendulum. Concerning the balancing of the pendulum, the angular position of the pendulum is to be controlled indirectly by means of the horizontal arm driven by the



**Table 1.** The control configuration.

Measured variables	$x_1, x_5$	Pendulum angle, electrical current
State variables	$x_1, x_2, x_3, x_4, x_5$	Angular positions and velocities of pendulum and horizontal arm; electrical current
Control variable	$\alpha$	Pendulum angle
Plant input and Disturbance	$e_d(t)$ and $M_{bp}(t)$	Applied voltage to the motor and moment created by exerted force to the pendulum by hand with a tap

motor, producing the control signal  $e_d(t)$  and applying it to the system, using appropriate control techniques.

### 3. Control of the system

A closed loop control system was designed and manufactured and many parameters of the pendulum system were determined experimentally. Simulation studies were executed with the real system parameters. In this study, since the control aim is to balance the pendulum at upright unstable position, only the angular position of the pendulum are measured and fed back. Control variable is the angular position of the pendulum and the inputs to the closed loop control system are the reference value of this angle and the disturbance (Table 1).

In simulations and experiments, several performance tests were carried out in order to show the dynamic behaviour of the plant and the efficiency of the control techniques utilized, which are PID control, SMC with *sat* saturation function and SMC with *tanh* sigmoid smoothing function.

#### 3.1. PID control

The PID control was tested only for experience and for further comparison studies, since it is the most classical control technique (KRi, 2015). The structure of the PID controller used in the computer program for control is as follows (Ogata, 1997).

$$u = K_p \left[ e(t) + K_i \int e(t) dt + T_d \frac{de(t)}{dt} \right] \quad (31)$$

where  $K_p$ ,  $K_i$  and  $T_d$  are the proportional, integral and derivative gains respectively, found by trial and error;  $u$  is the output of the controller. If  $u$  is multiplied by pre-amplifier gain ( $K_y$ ), the applied voltage is found as  $e_d(t) = K_y u$ . If  $K_i$  in equation (31) is tuned as zero, then control methods can be used as PD-control.

#### 3.2. Sliding mode control

SMC is a robust control technique being able to provide a desired dynamic behaviour in spite of

uncertainties in system model and disturbances (Rodriguez et al., 2006). “The most distinguished feature of VSC is its ability to result in very robust control systems; in many cases invariant control systems result. Loosely speaking, the term “invariant” means that the system is completely insensitive to parametric uncertainty and external disturbances ” (Hung et al., 1993).

Applying this technique to this study, using equations (20) and (21), dynamic behaviour of the plant with two degrees of freedom can be expressed as (Utkin, 1994; Rong and Özgüner, 2008).

$$M(q) \ddot{q} + f(q, \dot{q}, t) = \tau \quad (32)$$

where

$q$  : state vector,  $R_{2 \times 1}$

$M(q)$  : positive definite (square) mass matrix,  $R_{2 \times 2}$

$f(q, \dot{q}, t)$  : vector including centrifugal, Coriolis, gravity forces and the whole perturbation,  $R_{2 \times 1}$

$\tau$  : control torque vector,  $R_{2 \times 1}$

Taking  $q = p$  and  $\dot{q} = v$ , the motion equation can be written in the regular form as follows

$$\dot{p} = v \quad (33)$$

$$M(q) \dot{v} = -f(p, v, t) + \tau \quad (34)$$

The vector  $v$  considered as a control input can be stated with the following linear function of  $p$  in order to provide the desired dynamic behaviour as proposed by Utkin (1994):

$$v = -\lambda p \quad (35)$$

where  $\lambda$  is a positive scalar or a diagonal matrix including positive elements. Choosing the sliding surface as

$$s = v + \lambda p \quad (36)$$

and applying a discontinuous control input as

$$\tau = -M_0 \operatorname{sgn}(s) \quad (37)$$

with high enough positive  $M_0$  guarantees the existence of sliding mode in the manifold  $s=0$  with a resultant first order dynamic behaviour (Utkin, 1994).

$$\dot{p} = -\lambda p \quad (38)$$

As far as the stability of the control system is concerned, if the inequalities

$$\frac{1}{2} \frac{d}{dt} s^2 \leq -M_0 |s| \quad (39)$$

$$s \dot{s} \leq 0 \quad (40)$$

are satisfied, the designed control system will be stable (Utkin, 1977; Hung et al., 1993; Eker, 2006; Anvar et al., 2010; Chih-Jer et al., 2013; Kalaycı and Yiğit, 2015). Substituting  $\dot{s}$  with the switching input  $\tau$  into equation (40), the inequality

$$s[-M_0 \operatorname{sgn}(s)] \leq 0 \quad (41)$$

can be obtained. It can be easily seen that this condition for global stability will be satisfied for all first order sliding surfaces  $s(t)$ .

Switching control signal is usually used together with an equivalent control signal in SMC and it is obtained by means of system model. In case of no negative effects such as disturbances, uncertainties, parameter variations, etc. i.e. in ideal conditions, equivalent control signal can keep the system on the sliding surface. Hence, total control signal generally comprises “a switching control signal”  $u_{sw}$  [equals  $\tau$  in equation

(37)] plus “an equivalent control signal”  $u_{eq}$ , in the form of  $u = u_{sw} + u_{eq}$ .

In practice, during the application of the discontinuous control input, a zigzag motion called “chattering” occurs in sliding surface because of non-ideal switching and delayed system responses in sliding mode (Rong and Özgüner, 2008; Utkin, 1977).

“The ideal relay characteristic is practically impossible to implement, so one approach to reduce the chattering is to replace relay control by “continuous approximations” (Hung et al., 1993) like saturation function or tangent hyperbolic function as shown in Figure 3.

In order to reduce chattering, the following “saturation function” can be used instead of sign function and piecewise continuous control input as

$$\tau = -M_0 \operatorname{sat}(s/\varepsilon) \quad (42)$$

In order to reduce the chattering more, instead of  $\operatorname{sat}(s/\varepsilon)$ , a tangent hyperbolic (sigmoid) smoothing function  $\tanh(s/\varepsilon)$  can be preferred choosing a sufficiently small  $\varepsilon$  for a close vicinity of the sliding surface to create a continuous control input as

$$\tau = -M_0 \tanh(s/\varepsilon) \quad (43)$$

Boundary layer width of  $\varepsilon$  should be chosen high enough to reduce the chattering, but low enough not to eliminate robustness of the SMC, with a trial and error effort in practice (Hung et al., 1993; Eker, 2006; Anvar et al., 2010; Kalaycı and Yiğit, 2015).

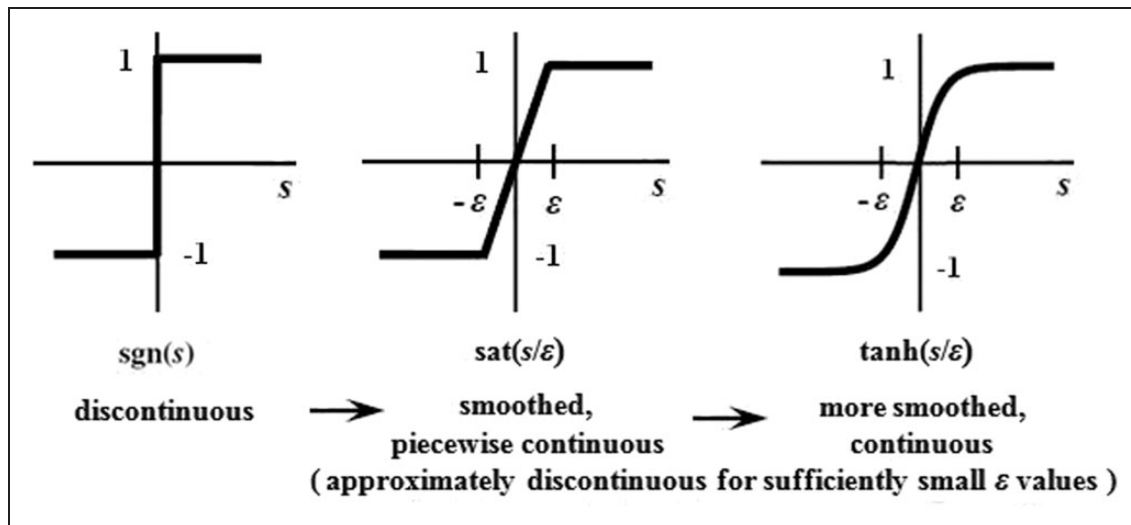


Figure 3. Switching functions for the “switching control input”.



**3.2.1. Stability analysis of the rotary inverted pendulum system.** State equations (26)–(30) represent the dynamic behaviour of the rotary inverted pendulum system in a standard form. For an easy stability analysis, servomotor dynamics (equation (30)) can be reduced to an algebraic statement as follows, by neglecting the terminal inductance of the servomotor, as in most cases for servomotors.

$$0 = -K_e x_2 - R_m x_5 + e_a(t) \quad (44)$$

Thus, the current through the motor bobbins ( $x_5$ ) can be obtained from equation (30) as

$$x_5 = \left( \frac{-K_e}{R_m} \right) x_2 + \left( \frac{1}{R_m} \right) e_a(t) \quad (45)$$

and substituting it into equation (27) and (29) gives a new form of state equations. These equations can be easily written in a standard mass matrix form as follows, as previously stated in equation (32).

$$M(q) \ddot{q} + f(q, \dot{q}, t) = \tau \quad (46)$$

From this point, all the stability analysis given by equations (32)–(41) are valid and can be applied to the rotary inverted pendulum system in a similar way.

As a result, the smoothing functions  $\text{sat}(s/\varepsilon)$  and  $\tanh(s/\varepsilon)$  can be assumed continuous approximations

of discontinuous (switching) function  $\text{sgn}(s)$  if the boundary layer width of  $\varepsilon$  is selected *sufficiently small* (Hung et al., 1993, Eker, 2006, Kalaycı and Yigit, 2015). Hence, with the approximately maintained discontinuity properties, it can be easily seen that the conditions  $s[-M_0 \text{sat}(s/\varepsilon)] \leq 0$  or  $s[-M_0 \tanh(s/\varepsilon)] \leq 0$  for the global stabilities will be satisfied for all first order sliding surfaces  $s(t)$  given by equation (36).

## 4. Experimental setup

The rotary inverted pendulum system developed in this study and its block diagram are shown in Figures 4 and 5, respectively. Some parameters of the servomotor used in the state equations were determined by experiments, since it was not possible to reach most of the technical specifications of the motor via producer information. A Celeron 600 PC equipped with a data acquisition and control card (Advantech 1710HG) with 12 bit resolution, 100000 samples/second sampling rate,  $\pm 1$  bit precision for all measurement ranges, and 5 microsecond conversion time was used for measurements as well as for the generation of the analog control signal. Since the control aim in this study is to balance the pendulum at upright unstable position, only the angular position of the pendulum is measured and fed back. Control variable is the angular position of the pendulum ( $\alpha$ ) from upright vertical position, which was measured using an angular position transducer.



**Figure 4.** Rotary inverted pendulum system (Bozok University, Department of Mechanical Eng., Mechatronics Lab).

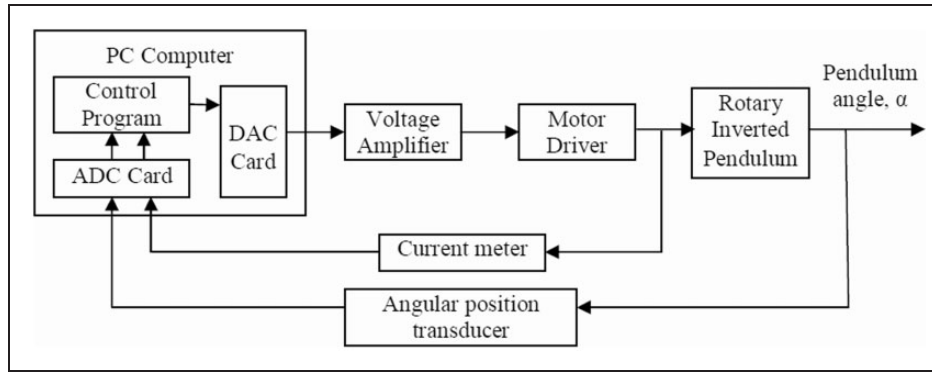


**Figure 5.** Block diagram of the rotary inverted pendulum system.

**Table 2.** Parameters of the system.

Dc servomotor specifications	Sperry electro components
Firm	
Nominal voltage*	25 volt
Stall current	$I_{max} = 4.0$ A for 20 volt input
Speed*	3000/11500 rpm
Torque constant	$K_t = 0.0384$ N.m/A
Back emf voltage	$K_e = K_t$ volt/(rad/s)
Mechanical time constant	$\tau_{mech} = 0.0048$ s
Electrical time constant	$\tau_{elek} = 0.0015$ s
Terminal resistance	$R_m = 8.6$ $\Omega$
Terminal inductance	$L_m = 0.0129$ Henry
Rotor inertia	$J_m = 8.2 \times 10^{-6}$ kg.m <sup>2</sup>
Friction torque (min.current $i_s = 0.33$ A)	$M_s = K_t i_s = 0.0126$ N.m
Friction constants and coefficients	
Coulomb friction constant (motor)	$M_{fa} = M_s$ N.m
Coulomb friction constant (pendulum)	$M_{fp} = 0.012015$ N.m
Damping coefficient (motor)	$B_a = 0.000366$ N.m.s/rad
Damping coefficient (pendulum)	$B_p = 0.001265$ N.m.s/rad
Masses, lengths and CGs of the links	$m_1 = 0.283$ kg, $m_2 = 0.127$ kg $r_{2x} = 0.05102$ m, $r_{2y} = 0$ m, $r_{2z} = 0.08093$ m, $L_2 = 0.300$ m
Moment of inertias (kg.m <sup>2</sup> )*	$I_{1z} = 0.00139306 + J_m$ $I_{2x} = 0.00012007$ $I_{2y} = 0.00149364$ $I_{2z} = 0.00029395$ $I_{2xz} = I_{2zx}$ $= 0.00026739$ (Other elements of the inertia matrix are zero)
Angular position transducer *	GEFRAN, $\pm 0.05\%$ volt, 4.7 K $\Omega$

All parameters were experimentally found except for those designated by means of \*technical properties and \*\* software packages.

In the light of the simulation results, a rotary inverted system was designed and manufactured. Parameter values of the rotary inverted pendulum system are summarized in Table 2. As given in Table 2, some of the parameters were taken from technical properties of the products (designated as “\*technical properties”), some were obtained by using software packages (designated as “\*\* software packages”), and most of them were determined

experimentally. Simulation studies were repeated with these real system parameters.

## 5. Results and discussion

Simulation studies were implemented with the real system parameters determined experimentally. A great number of simulations were carried out by repeating the same test with the same operating conditions, but

for different controllers and controller tuning parameters. Since the control aim in this study is to balance the pendulum at upright unstable position, only the angular position of the pendulum is measured and fed back. Control variable is the angular position of the pendulum and inputs to the closed loop control system are reference value of this angle and the disturbance. Several performance tests were carried out in order to show the dynamic behaviour of the plant and the efficiency of the control techniques utilized, namely PD, PID control, SMC with *sat* saturation function and SMC with *tanh* sigmoid smoothing function.

During experiments and simulations, in all cases, initial positions of the pendulum angles were about 30 degrees from vertical direction and other initial values of the state variables were zero. Moment disturbances of about 0.035 N.m were created roughly by applying a force by hand with a screwdriver.

In simulations, the same real amounts of deviations in pendulum angles due to disturbances were approximately satisfied with the values mentioned above that are obtained by comparing the responses in the experiments and simulations. Otherwise, it is hardly possible to measure the disturbances.

### 5.1. PID control

Several simulations and experiments were carried out by applying PID and PD control. A typical simulation result for PD control is given as an example in Figure 6 and typical experimental results obtained for PID-control with  $K_p=100$  and  $K_i=0.001$  and  $T_d=0.002$  and PD-control with  $K_p=100$  and  $K_i=0$  and  $T_d=0.002$  are given in Figures 7 and 8, respectively. It was observed from the experiments that, unlike in simulations, the system was controlled better by using PD control than PID. Even if a small amount of I-control was added, i.e., making it PID, the system exhibits more oscillatory responses with lower dynamic stiffness. Increasing the proportional gain results in an oscillatory response again but contributes to regulation properties of the system against disturbances.

The responses given in Figures 6–8 indicate that using PD or PID control is not sufficient for an accurate control of the rotary inverted pendulum. The figures also show that disturbances were not compensated for satisfactorily, which were manually performed on the pendulum in balance condition.

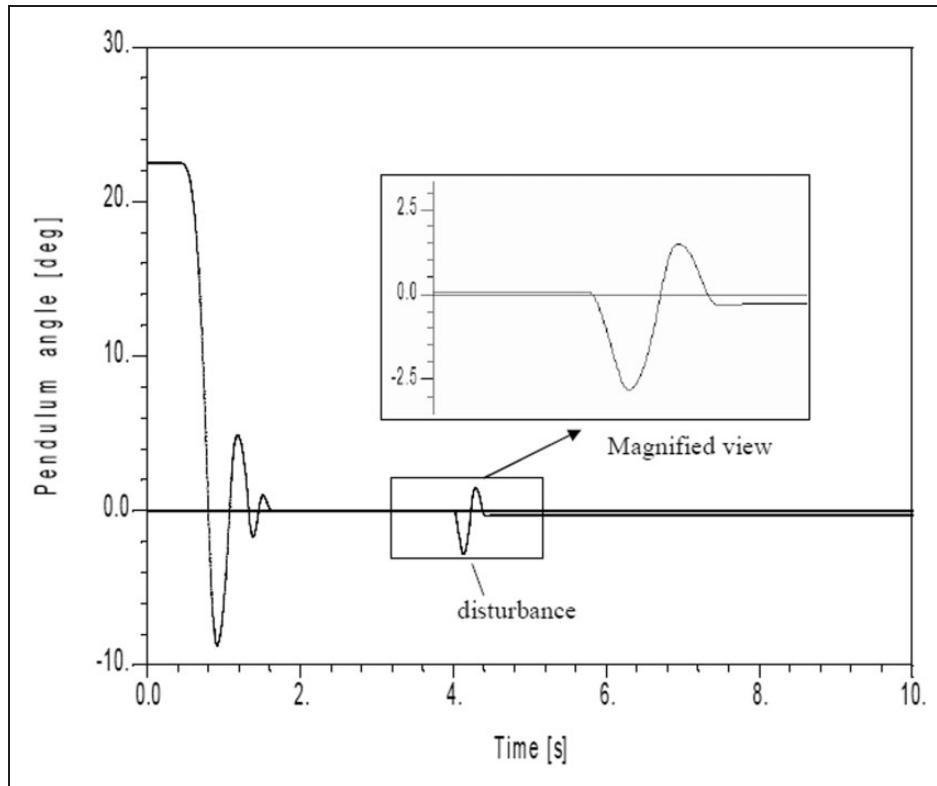


**Figure 6.** Response to step reference angle of pendulum (simulation) (PD Control:  $K_p = 150$  and  $K_i = 0$  and  $T_d = 0.002$ ).

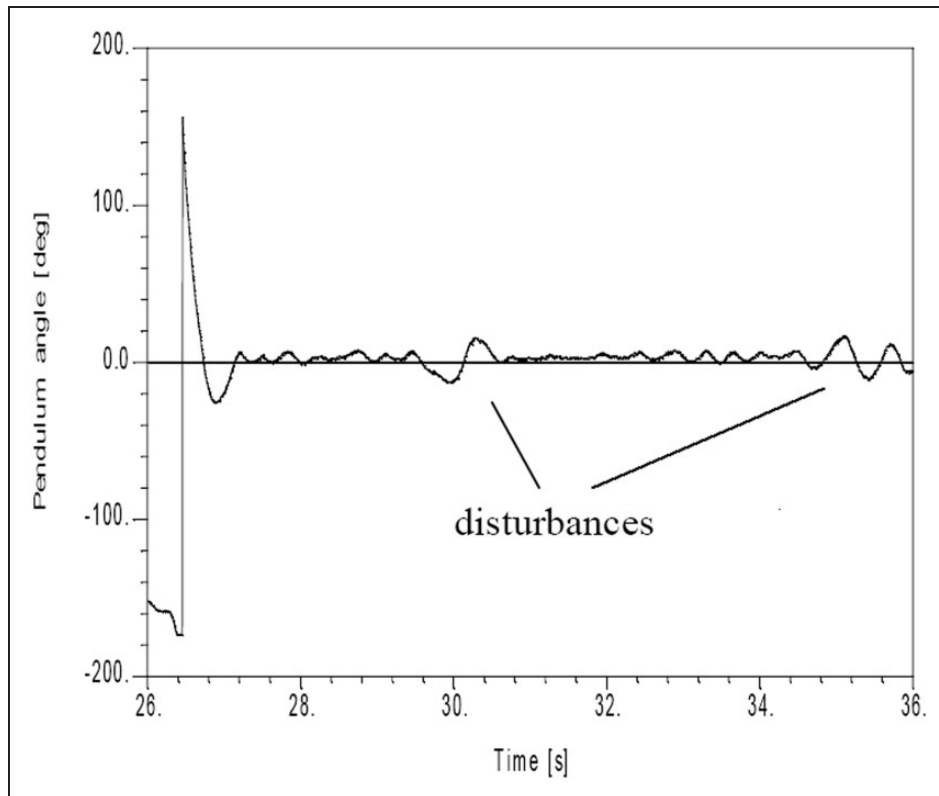


**Figure 7.** Response to step reference angle of pendulum (experiment) (PID-control with  $K_p = 100$  and  $K_i = 0.001$  and  $T_d = 0.002$ ).

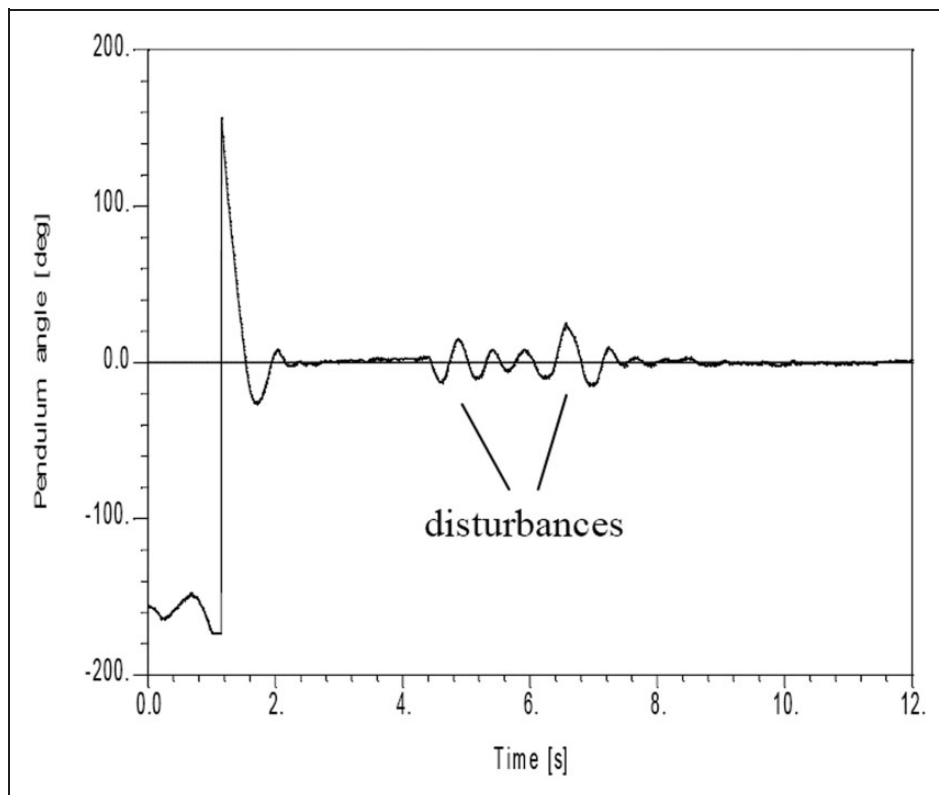


**Figure 8.** Response to step reference angle of pendulum (experiment) (PD-control with  $K_p = 100$  and  $K_i = 0$  and  $T_d = 0.002$ ).

## 5.2. Sliding mode control

SMC technique generally necessitates all state variables by means of measurements or observations, causing an increase in sampling rate in the control program. In most cases, it is impossible, costly, or time-consuming to obtain these variables. In simulations and experimental studies, it is assumed that only the pendulum angle was measured and fed back; the angular speed was included indirectly by derivation of the angular position error. Hence, a first order sliding surface (as in equation (36)) was preferred in SMC of the system, using the angular position error of the pendulum ( $e = \alpha_{ref} - \alpha$ ) and its time derivative as

$$s = \dot{e} + \lambda e \quad (47)$$

Several simulations and experiments were implemented using SMC with saturation function  $\text{sat}(s)$  with a wide range of  $\lambda$  gains. In order to reduce the chattering more, instead of  $\text{sat}(s/\varepsilon)$ , sigmoid smoothing function  $\tanh(s/\varepsilon)$  was preferred with a sufficiently small interval of  $[-\varepsilon, \varepsilon]$ . In all cases, the value of  $\varepsilon$  was chosen high enough to reduce the chattering, but low enough not to eliminate robustness of the SMC, with a trial and error method.

**5.2.1. Sliding mode control with saturation smoothing function.** Several simulations and experiments were implemented using SMC with  $\text{sign}(s)$  switching function with a wide range of  $\lambda$  gains. During the studies, it was observed that the greater the gain  $\lambda$  was increased the more oscillatory or vibratory behaviour (chattering) was obtained. In order to reduce the chattering, saturation smoothing function of  $\text{sat}(s/\varepsilon)$  was used instead of  $\text{sign}(s)$  function. For example, a typical simulation result obtained for  $\lambda = 100000$  &  $\varepsilon = 15$  and a typical experimental result obtained for  $\lambda = 100000$  &  $\varepsilon = 2000$  are given in Figures 9 and 10, respectively.

**5.2.2. Sliding mode control with sigmoid smoothing function.** In order to reduce the chattering more,  $\tanh(s/\varepsilon)$  was used instead of  $\text{sat}(s/\varepsilon)$  in a sufficiently small interval of  $[-\varepsilon, \varepsilon]$ . The responses of the system to zero step reference angles with a wide range of  $\lambda$  and  $\varepsilon$  values were obtained.

Typical simulation results with  $\tanh(s/\varepsilon)$  for  $\lambda = 200000$  &  $\varepsilon = 15$  and  $\lambda = 200000$  &  $\varepsilon = 20$  are given as examples in Figures 11 and 12, respectively.

Several experiments were conducted using  $\tanh$  smoothing function and a typical response for  $\lambda = 200000$  &  $\varepsilon = 2000$  is given in Figure 13.

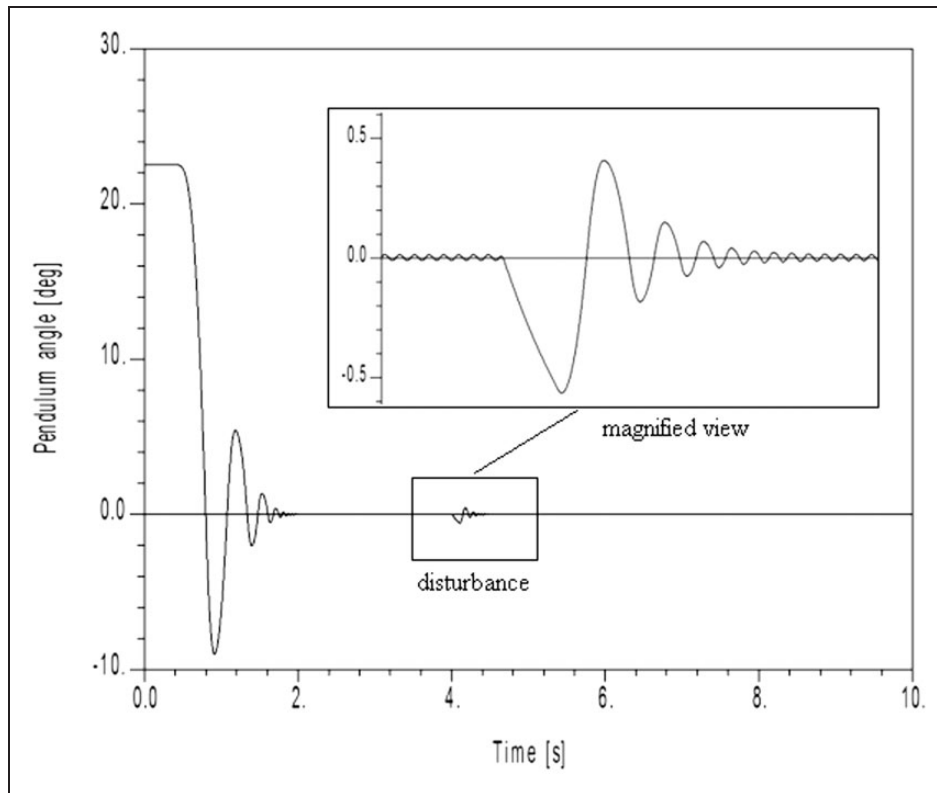


**Figure 9.** Response to step reference angle of pendulum (simulation) (SMC with  $\text{sat}(s/\varepsilon)$  saturation function:  $\lambda = 100000$  &  $\varepsilon = 15$ ).

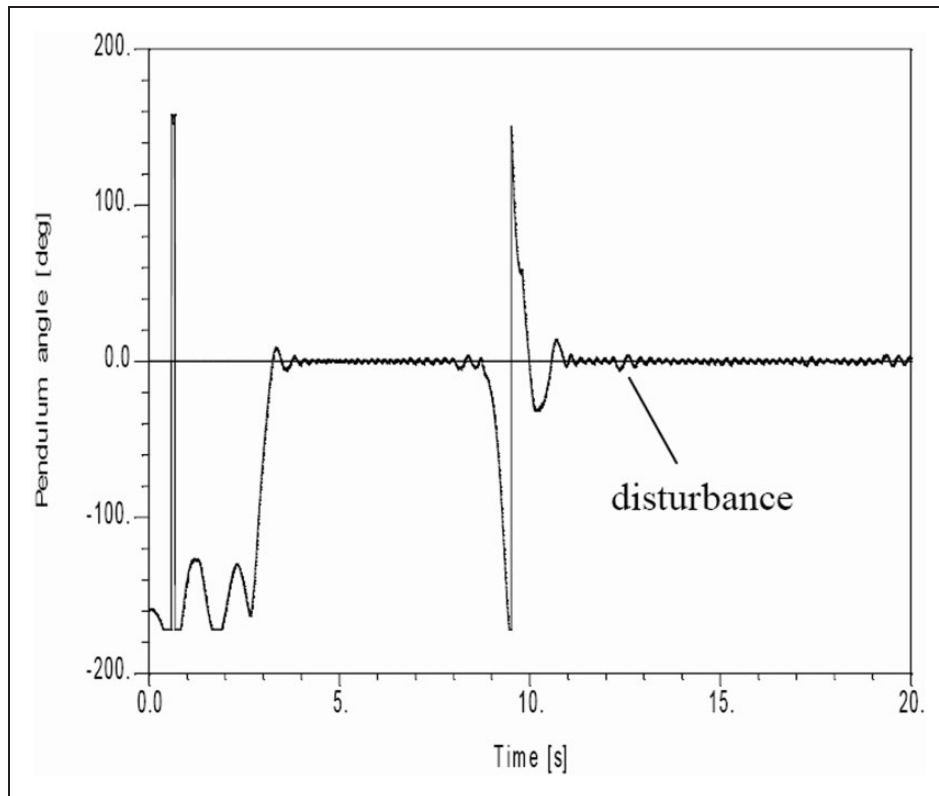


**Figure 10.** Response to step reference angle of pendulum (experiment) (SMC with  $\text{sat}(s/\varepsilon)$  saturation function:  $\lambda = 50000$  &  $\varepsilon = 10$ ).

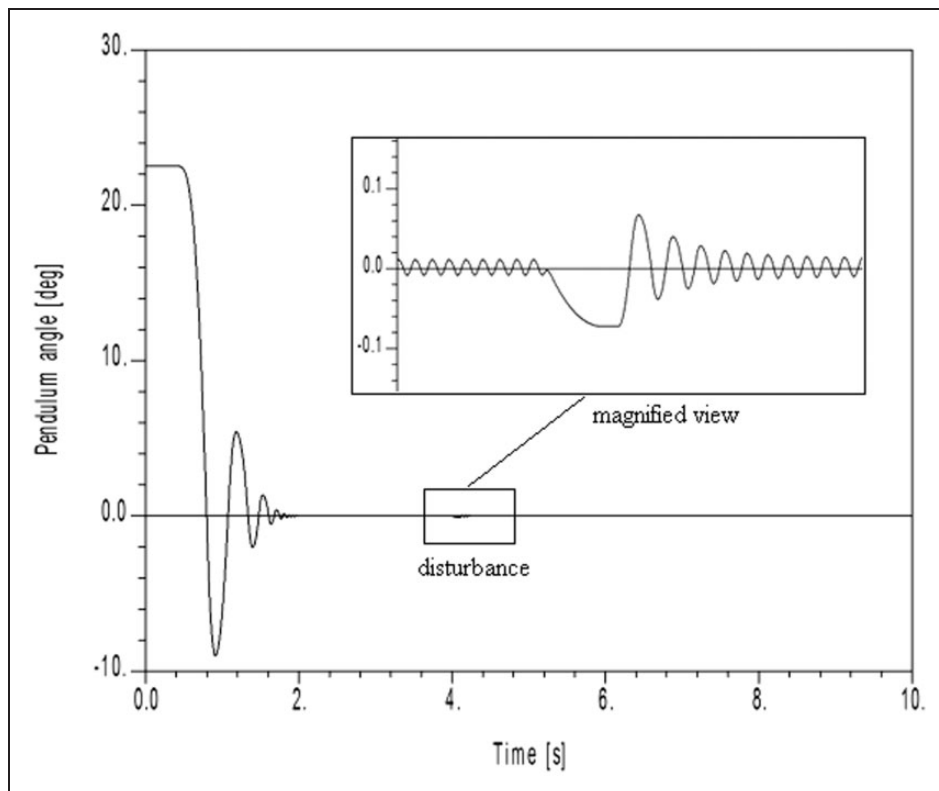


**Figure 11.** Response to step reference angle of pendulum (simulation) (SMC with  $\lambda = 100000$ ,  $\varepsilon = 15$  with  $\tanh(s/\varepsilon)$  sigmoid function).



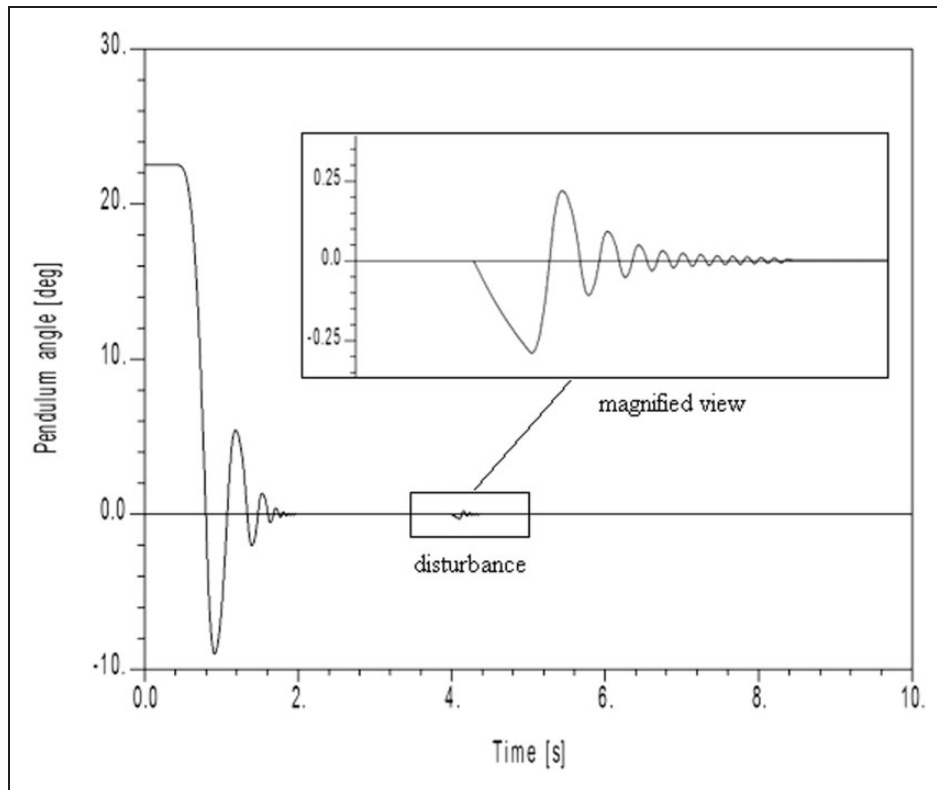


**Figure 12.** Response to step reference angle of pendulum (simulation) (SMC with  $\lambda = 100000$ ,  $\varepsilon = 20$  with  $\tanh(s/\varepsilon)$  sigmoid function).

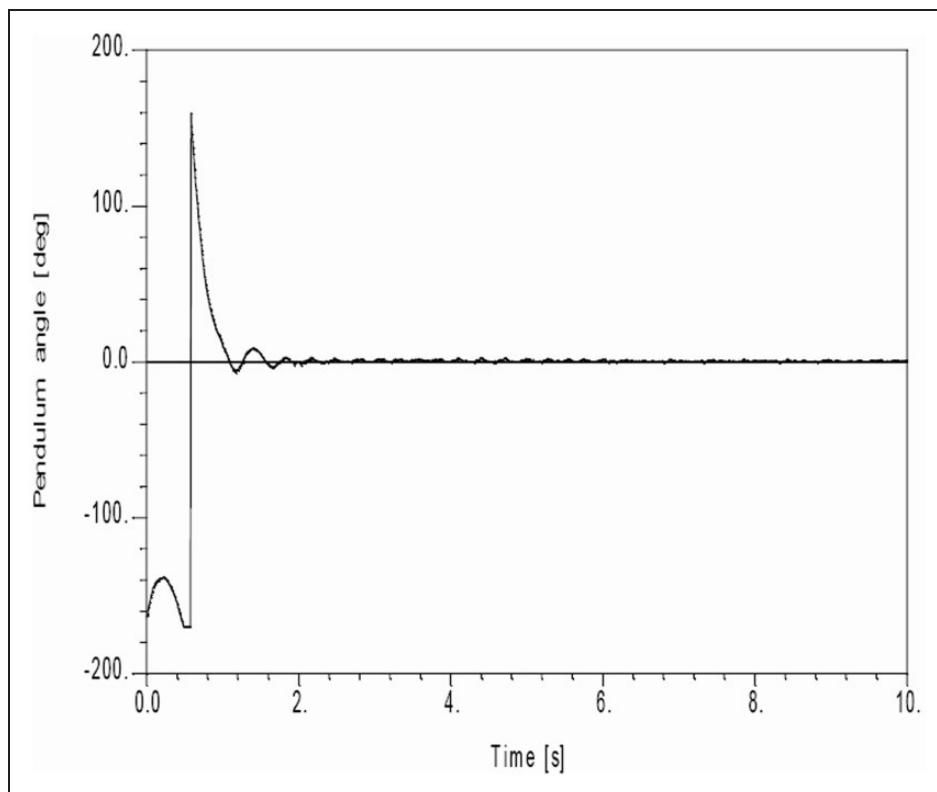


**Figure 13.** Response to step reference angle of pendulum (experiment) (SMC with  $\lambda = 100000$ ,  $\varepsilon = 2000$  and  $\tanh(s/\varepsilon)$  sigmoid function).

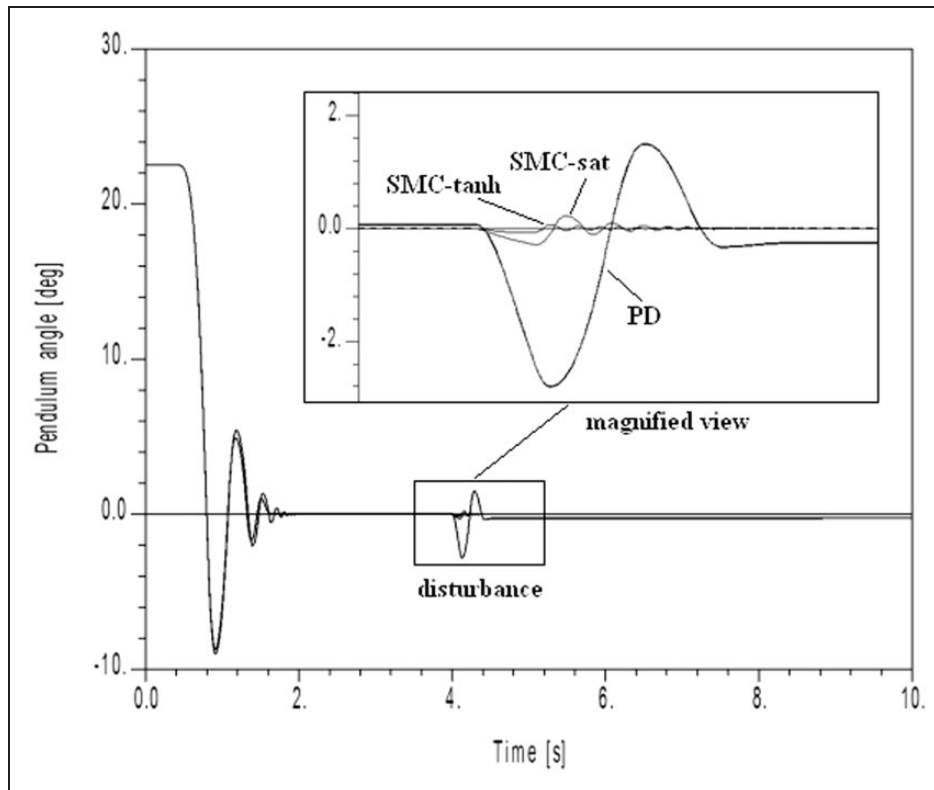


**Figure 14.** Comparison of the control methods (simulation) (PD, SMC-sat( $s/\epsilon$ ) and SMC- tanh( $s/\epsilon$ )).

As shown in Figures 11–13, the chattering reduced more, along with a very low steady state error. It was observed from the experiments that robustness increased to a certain level compared to the control with sat( $s/\epsilon$ ) function. In experiments,  $\epsilon = 20$  was not big enough to reduce chattering more because of unmodelled nonlinear parasitic effects, such as noise, switching delay, hysteresis, stiction, etc. Therefore, value of  $\epsilon$  was increased to an amount of  $\epsilon = 2000$ .

**5.2.3. Comparison of the control methods.** It is shown in Figures 6 to 13 that simulation results are in accordance with experimental results. As such, to compare the control methods (PD, SMC-sat( $s/\epsilon$ ) and SMC-tanh( $s/\epsilon$ )), responses to step reference angle of the pendulum obtained from simulations were given in a frame in Figure 14. It was observed from simulation and experimental studies that changes from catching to upright position occurred with a deviation of about  $\pm 30$  degrees of pendulum angle for all control techniques experienced and no significant difference was seen among them.

It is also observed that using PD is better than PID for the control of the system, but both PD and PID controls are not sufficient for an accurate control of the rotary inverted pendulum and they do not compensate for the disturbances satisfactorily.

In SMC-sat( $s/\epsilon$ ), the results indicate that the chattering was reduced, but an amount of decrease was observed in the robustness. In case of using SMC-tanh( $s/\epsilon$ ) instead of sat( $s/\epsilon$ ), as shown from the results, the chattering reduced more, along with a low steady state error. Using sigmoid smoothing function, the system exhibits more robust responses, regulates disturbances quicker, catches the pendulum about the reference angle easier than those obtained in SMC with saturation function only. The most prominent advantage of using SMC with sigmoid smoothing function tanh( $s/\epsilon$ ) is clearly observed.

Comparison of the steady state values measured from the responses to step reference angle of the pendulum is given in Figure 15. As shown in the figure, SMC with sigmoid function exhibits the least steady state error as been expected.

Overall performances of the control techniques used are given in Table 3. As shown in the table, SMC with sigmoid smoothing function gives the best results of all.

## 6. Conclusion

In the study, nonlinear modelling, simulation and model free sliding mode stabilizing control of a real rotary inverted pendulum were dealt with in detail.

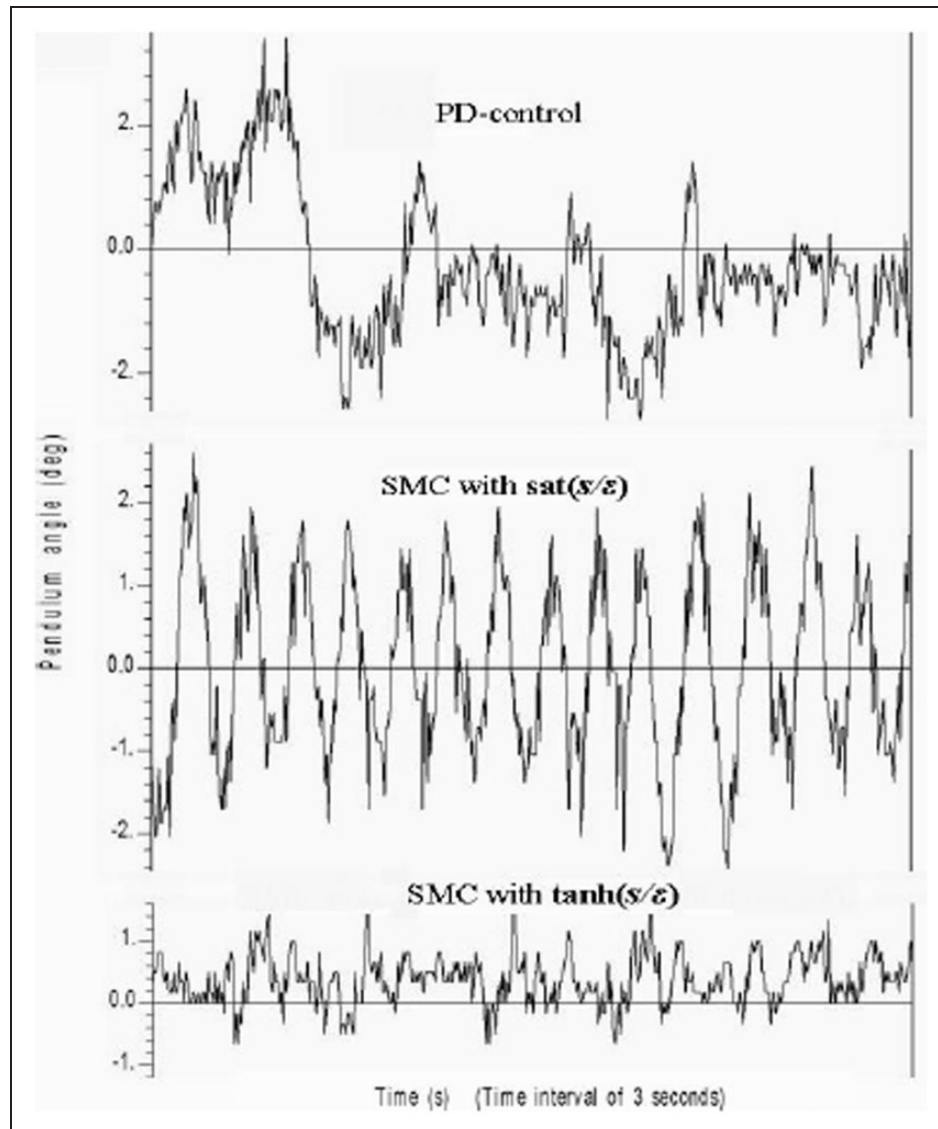


**Figure 15.** Comparison of the steady state values (experiment) (responses to step reference angle of the pendulum).

**Table 3.** Comparison of the overall performances of the control techniques used.

Approximated values	Overshoot (%)	Settling time (s)	Steady state value ( $\pm$ deg)	Chattering ( $\pm$ deg)	Robustness (based on 100p.)
PD control	25	1	3	—	70
PID control	20	2	2	—	50
SMC-sat( $s/\epsilon$ )	10	1	2	2	90
SMC-tanh( $s/\epsilon$ )	5	2	1	1	100

The system was modelled in a nonlinear state space form including the servomotor dynamics. In the light of the simulation results, a closed loop control system was designed and manufactured and parameters of the pendulum system were determined experimentally. For

a certain quality level of output, benefits of the sliding mode control of the system without using an equivalent control signal by selecting a proper smoothing function were shown. Comparisons of the theoretical and experimental results show that the state equations describe

the dynamic behaviour of the system satisfactorily, and that robust and accurate balancing of the pendulum can be achieved by using model free SMC with sigmoid smoothing function. This model free approach can be used to meet a need especially for practical control applications in industry to a certain level. This concluding result is obtained from a practical point of view based on focusing merely on desired quality levels in system responses. It is expected that this approach will encourage practical control engineers to use SMC, who have no ability to model a system or no sufficient time for this, or encounter very complex nonlinear system models in many cases.

### Acknowledgements

Bozok University Faculty of Engineering and Architecture and my dear family are gratefully acknowledged.

### Conflict of interest

The author declared no potential conflicts of interest with respect to the research, authorship, and/or publication of this article.

### Funding

The author received no financial support for the research, authorship, and/or publication of this article.

### References

- Anvar, SMM, Hassanzadeh I and Alizadeh G (2010) Design and implementation of sliding mode-state feedback control for stabilization of rotary inverted pendulum. In: *ICCAS 2010-International Conference on Control, Automation and Systems*. pp. 1952–1957.
- Åström KJ and Furuta K (2000) Swinging up a pendulum by energy control. *Automatica* 36: 287–295.
- Awtar S, King N, Allen T, et al. (2002) Inverted pendulum systems: rotary and arm-driven-A mechatronics system design case study. *Mechatronics* 12: 357–370.
- Berg Van Den HWJ (2003) Introduction to the control of an inverted pendulum setup. Report: *Eindhoven University of Technology*. Report no. 2003.56.
- Chih-Jer L, Chih-Keng C and Kai-Sheng L (2003) Implementation of an extended sliding mode control for a rotational invert pendulum's Tracking Problem with Output Feedback. *J Chinese Soc Mech Eng* 24: 277–282.
- Eker İ (2006) Sliding mode control with PID sliding surface and experimental application to an electromechanical plant. *ISA Transactions* 45: 109–118.
- Fridman L (2012) Sliding Mode Enforcement after 1990: Main Results and Some Open Problems. In: Moreno J and Iriarte R (eds.) *Sliding Modes after the first Decade of the 21st Century, Lecture Notes in Control and Information Sciences*. Berlin: Springer Verlag, pp. 1–79.
- Hung JY, Gao W and Hung JC (1993) Variable structure control: A survey. *IEEE Trans. Industrial Electronics* 40: 2–22.
- Kalaycı MB and Yiğit İ (2015) Theoretical and experimental investigation of some sliding mode control techniques used in practice. *J. Fac. Eng. Arch. Gazi Univ.* 30: 131–142.
- Khanesar MA, Teshnehlab M and Shooehdeli MA (2007) Sliding mode control of rotary inverted pendulum. In: *IEEE Mediterranean Conference on Control and Automation*. pp. 1–6.
- KRi (KentRidge Instruments Pte. Ltd.) (2015) *Inverted Pendulum Apparatus PP-300*. Available at: <http://www.kri.com.sg/pend.html#Theory>
- Ogata K (1997) *Modern Control Engineering*. Upper saddle river (NJ): Prentice Hall.
- Olfati-Saber R (2000) Cascade normal forms for underactuated mechanical systems. In: *Proceedings of the 39th IEEE Conference on Decision and Control*. pp. 2163–2167.
- Pakdeepattarakorn P, Thamvechvitee P, Songsiri J, et al. (2004) Dynamic models of a rotary double inverted pendulum system. In: *Proceeding of IEEE Region 10 Conference on Analog and Digital Techniques*, pp. 558–561.
- Rodriguez MT, Banks SP and Salamci MU (2006) Sliding Mode Control: An Iterative Approach. In: *45th IEEE Conference on Decision and Control*. pp. 4963–4968.
- Rong X and ÖzgünerÜ (2008) Sliding mode control of a class of underactuated systems. *Automatica* 44: 233–241.
- Trivedi PK and Bandyopadhyay B (2010) Non unique equivalent control in sliding mode with linear surfaces. In: *IEEE ICPCES Int. Conference on Power, Control and Embedded Systems*. pp. 1–5.
- Usai E (2008) Sliding mode: Basic theory and new perspectives. In: *SDS2008 5th Workshop on Structural Dynamical Systems: Computational Aspects*. pp. 1–54.
- Utkin VI (1992) *Sliding Modes in Control and Optimization*. Germany: Springer-Verlag.
- Utkin VI (1994) Sliding mode control in mechanical systems. In: *IEEE IECON'94, 20th International Conference on Industrial Electronics, Control and Instrumentation*. pp. 1429–1431.
- Utkin VI (1977) Variable structure systems with sliding modes. *IEEE Trans. Automatic Control* 22: 21–222.